Developmental Biology 360 (2011) 403–414

Contents lists available at SciVerse ScienceDirect

Developmental Biology

journal homepage: www.elsevier.com/developmentalbiology

Second order regulator Collier directly controls intercalary-specific segment polarity gene expression

Evgenia Ntini, Ernst A. Wimmer *

Department of Developmental Biology, Johann-Friedrich-Blumenbach-Institute of Zoology und Anthropology, Georg-August-University Göttingen, GZMB, Ernst-Caspari-Haus, Justus-von-Liebig-Weg 11, 37077 Göttingen, Germany

ARTICLE INFO

Article history:
Received for publication 27 June 2011
Revised 28 September 2011
Accepted 29 September 2011
Available online 8 October 2011

Keywords:
Cis-regulatory element
Head development
Metamerization
Segmentation
Transcriptional control

ABSTRACT

In *Drosophila*, trunk metamerization is established by a cascade of segmentation gene activities: the gap genes, the pair rule genes, and the segment polarity genes. In the anterior head, metamerization requires also gap-like genes and segment polarity genes. However, because the pair rule genes are not active in this part of the embryo, the question on which gene activities are fulfilling the role of the second order regulator genes still remains to be solved. Here we provide first molecular evidence that the Helix–Loop–Helix–COE transcription factor Collier fulfills this role by directly activating the expression of the segment polarity gene *hedgehog* in the posterior part of the intercalary segment. Collier thereby occupies a newly identified binding site within an intercalary-specific *cis*-regulatory element. Moreover, we identified a direct physical association between Collier and the basic-leucine-zipper transcription factor Cap'n'collar B, which seems to restrict the activating input of Collier to the posterior part of the intercalary segment and to lead to the attenuation of *hedgehog* expression in the intercalary lobes at later stages.

Introduction

The metameric expression pattern and the functional role of segment polarity genes in segmentation are highly conserved across the animal kingdom (Chipman and Akam, 2008; Damen, 2002; Dray et al., 2010; Holland et al., 1997; Patel, 1994). Also the metamerization of the insect head involves segment polarity genes whose expression patterns clearly demark anterior segments (Rogers and Kaufman, 1996; Schmidt-Ott et al., 1994b). However, in *Drosophila melanogaster* it was recognized that head development does not follow the well analyzed mode of trunk segmentation which employs the hierarchical cascade of maternal coordinate genes, gap, pair rule, and segment polarity genes (St Johnston and Nüsslein-Volhard, 1992), while specification of segment identity is accomplished by the *Hox* genes (McGinnis and Krumlauf, 1992). The labial and maxillary segments of the posterior head region—part of the gnathocephalon—are patterned according to this trunk segmentation mode, and the mandibular gnathal segment integrates regulatory inputs from both the head and trunk patterning systems (Cohen and Jürgens, 1991; Grossniklaus et al., 1994; Vincent et al., 1997; Wimmer et al., 1997). Metamerization and segment identity specification in the anterior head region—the procephalon—resulting in formation of the intercalary, antennal and ocular segments, however, takes place in the absence of pair rule and *Hox* gene activity (Cohen and Jürgens, 1991; Finkelstein and Perrimon, 1991).

The metamerization process of the anterior head region employs the activities of the head gap-like genes *orthodenticle* (*otd*), *empty-spiracles* (*ems*) and *buttonhead* (*btd*) which are expressed early in embryogenesis in broad and overlapping domains (Wimmer et al., 1997) and are necessary for the cephalic segmental expression patterns of segment polarity genes (Cohen and Jürgens, 1990; Mohler, 1995; Rogers and Kaufman, 1997; Schmidt-Ott et al., 1994a). Phenotypic analysis of head gap-like mutants *otd*, *ems*, and *btd* indicated that each gene is necessary for a partially overlapping block of two to three segments with their posterior functional limit being out of phase by one segment (Cohen and Jürgens, 1990; Schmidt-Ott et al., 1994a). The lack of pair rule and *Hox* gene activity in this anterior head region led to the hypothesis that the segmental out-of-phase expression of the head gap-like genes is responsible for the metamerization whereas the different combination of their expression is responsible for the segment identity (Cohen and Jürgens, 1991). However, ectopic expression studies with *btd* (Wimmer et al., 1997) and *otd* (Gallitano-Mendel and Finkelstein, 1998) showed that neither the expression borders are instructive for setting up metamerization nor the combinatorial code is responsible for segment identity. Only in the case of ectopic expression of *ems* a homeotic transformation of the mandibular segment into a second intercalary segment was observed (Schöck et al., 2000). The intercalary segment is actually the anterior-most segment expressing a *Hox* gene—*labial*—(Abzhanov and Kaufman, 1999), for which, however, no clear evidence exists that it provides homeotic selector gene activity in the *Drosophila* embryo (Merrill et al., 1989). The segment identity of the mandibular segment is essentially controlled by the basic-leucine-zipper (bZIP) transcription factor encoding gene *cap'n'collar* (*cnc*) (Mohler et al., 1995), since the isoform CncB alters the function of

* Corresponding author. Fax: +49 551 39 5416.
E-mail address: ewimmer@gwdg.de (E.A. Wimmer).

0012-1606/$ – see front matter © 2011 Elsevier Inc. All rights reserved.
doi:10.1016/j.ydbio.2011.09.035

the *Hox* gene *Deformed* that by itself promotes maxillary structures (McGinnis et al., 1998; Veraksa et al., 2000).

The head gap-like genes *otd*, *ems*, and *btd* are necessary for the early, broad and overlapping blastodermal expression patterns of the segment polarity genes *hedgehog* (*hh*) and *wingless* (*wg*) and it was proposed that the regulatory interactions between the segment polarity genes would then be responsible for their later metameric expression pattern (Mohler, 1995). However, genetic analysis of cross-regulations between segment polarity genes revealed that the metameric expression of one segment polarity gene does not rely on the function of another segment polarity gene in the anterior head region (Gallitano-Mendel and Finkelstein, 1997). Thus, at the lack of pair rule gene activity, it is still largely unknown how the patterning information is transmitted from the head gap-like genes to the segment polarity genes in the anterior head region. In this context, the isolation and phenotypic analysis of mutations in the gene *collier/knot* (*col*) indicated a parasegment (PS)-specific patterning gene acting downstream of the head gap-like genes in the head, as a second-order regulator similar to the pair rule genes in the trunk (Crozatier et al., 1996, 1999). *col* encodes a Helix–Loop–Helix (HLH) member of the COE (Collier/Olfactory-1/Early B-Cell Factor) transcription factor family (Crozatier et al., 1996; Daburon et al., 2008; Jackson et al., 2010), is expressed in PS0 (consisting of the posterior part of the intercalary segment and the anterior part of the mandibular segment), and is required for the establishment of *hh* expression in the posterior part of the intercalary segment (Crozatier et al., 1999). In this study we provide molecular evidence that this regulatory genetic interaction between Collier and *hh* is accomplished by direct activation at the transcriptional level.

In order to elucidate the gene networks of anterior head patterning, we previously employed a bottom-up approach by dissecting and functionally assaying *cis*-regulatory regions of segment polarity genes (Ntini and Wimmer, 2011). In that analysis an intercalary-specific *cis*-regulatory element of *hh* (*ic-CRE*) was identified. Here we report that Collier activates *hh* expression in the posterior part of the intercalary segment by occupying a newly identified essential binding site within this *ic-CRE*. This data further supports the function of second-order regulators in the patterning process of the anterior head region. Moreover, we detected a physical protein interaction between Collier and CncB. We propose that this interaction restricts the activating input of Collier to the posterior part of the intercalary segment by prohibiting downstream target activation in the anterior part of the mandibular segment where the two factors are co-expressed, and it might also be responsible for the late attenuation of *hh* expression in the intercalary lobes.

Materials and methods

Whole mount embryo in situ hybridization

cDNAs were cloned in PCRII (Invitrogen) and antisense-RNA was generated from T7 or Sp6 promoter using the respective RNA polymerase (Roche). *In vitro* transcription was in the presence of 10% DIG- or Fluo-labeling rNTP mix (Roche). 0–10,5 h embryo collections were dechorionated for 3 min in 50% chlorix, and fixed (20 min@rt) in [2 ml heptane, 3.7% formaldehyde in 1.5 ml PEM (0.1 M PIPES, 1 mM MgCl2, 1 mM EGTA pH 6.9)]. Double *in situ* hybridization was as in Rehm et al. (2009), apart from an additional 30 min treatment in (1% SDS, 0.5% Tween-20, 50 mM Tris–HCl pH 7.5, 1 mM EDTA, 150 mM NaCl) before prehybridization. NBT/BCIP staining was in AP buffer pH 9.5 and FastRed staining in AP buffer pH 8.2.

Transgenesis

For site-specific transgenesis using the *attB–attP φC31*-mediated integration system (Bischof et al., 2007), reporter cassettes consisting of [*cis*-regulatory region_*hh* promoter (−120_+99 bp)_*tGFP-SV40*] were excised with AscI from *pslaf_tgfp_af.2* and subcloned in the AscI site of the *pBac_attB* vector (Ntini and Wimmer, 2011). The line injected was the one bearing the *attP* landing site at position 96E of the 3rd chromosome (Ac. Num EF362408). This is a combined line carrying on the X chromosome a codon-optimized *φC31* integrase driven under the control of the *vasa* promoter (Bischof et al., 2007).

Chromatin immunoprecipitation followed by quantitative real-time PCR

Chromatin immunoprecipitation was after Sandmann et al. (2006). The following are noted in addition: The isolated nuclei were sonicated using a Bioruptor sonicator (Diagenode) at medium settings (15 s on/15 s off, total 20 min). In the ChIP reaction 10 μg of antibody (mouse-a-Col or mouse-a-BP102 in the mock IP) were added at a volume dilution 1:100. Enrichment of the Col binding site in the IP samples was assessed by qPCR using target primers ATCCATCCATTTGCCTAATTTCT, F and CTGTGTTCAGGCTGTTTAATTCAC, R (amplicon −3804 to −3716 bp *hh*). Negative control primers amplifying 111 bp within the second exon of *caudal* were GAGCTGGAGAAGGAGTACTGCAC, F and CGGTTCTGGAACCAGATCTTAAC, R. Primers were designed using the program Primer3 (http://frodo.wi.mit.edu/primer3/) with the parameters: Amplicon size 75–150 bp, Minimum primer Tm 59 °C, Optimal 60 °C, Maximum 62 °C and maximum Tm difference within the primer set 0.5 °C. qPCR reactions in 15 μl (1xSYBR Green I Master Mix (BioRad), 0.5 μl of each primer) were set in triplets, using the Chromo4 cycler and software (BioRad) and the program: 10 min 95 °C (Hot Start) and 40 cycles of (15 s 95 °C denaturation and 1 min 60 °C annealing/extension).

In vitro protein expression

Coding sequences of the complete open reading frames were isolated by proofreading PCR (Fermentas) on a 0–12 h embryonic cDNA pool (SMART PCR cDNA Synthesis Kit, ClonTech). ColA was isolated with primers GCTTCAAGCTGCGTTCCGAAGAG (F), GGGCCTGCCAATAGCCTCATTTAGTAG (R). ColB with ATGGAGTGGGGCCGGAAGCTGTA (F), GGGAGTCCGGGAAATGCTTAAACG (R). CncB with CTCGAGACGAGATGTTGCAATCAGCGGTTC (F) GAATTCATTCCTTGCGGTGCTGCTGTTGC (R). cDNAs were cloned in pTNT (Promega). 8.5 μg of recombinant plasmid DNA was used as template in *in vitro* transcription and translation reaction using the TNT Wheat Germ Cell SP6 System (Promega). A mock reaction was performed by using as template 8.5 μg of empty pTNT vector. Efficiency of protein expression was checked by subjecting 1 μl of the TNT reaction to 8% SDS PAGE followed by immunoblotting.

Electrophoretic mobility shift assay

Upper and lower strands spanning the DNA binding site were ordered as HPLC purified, partially overlapping complementary oligos. These were annealed leaving 3′ overhangs of 3–8 nucleotides in the double stranded form to be filled in by Klenow (3′–5′ exo$^-$) (New England BioLabs, NEB). 200 ng of ds oligo template was subjected to Klenow labeling reaction [0.25 mM d[A,G,T]TP, 10 μCi [α-^{32}P]dCTP (800 Ci/mmol)]. The generated probe was passed through a G25 column (GE Healthcare) to eliminate presence of unincorporated nucleotides. 150 cps (0.05–0.15 pmol) of probe were used per EMSA reaction. EMSA binding reactions were set in a final volume of 20 μl including 1x Binding Buffer (10 mM Hepes pH 7.9, 60 mM KCl, 8.4% glycerol, 1 mM EDTA, 2.5 mM MgCl2, 1 mM DTT, 0.2 μM ZnAc,). 0.5–4.5 μl of TNT Wheat Germ Cell SP6 System (Promega) expressed protein was added in the presence of poly dI–dC (Amersham) (100 ng/μl) prior to the probe. The binding reactions were incubated at room temperature for 30 min. For supershift reactions the protein factor was preincubated with 0.5–1 μl of anti-Col for 20 min at room temperature before adding the probe. Reactions were loaded on a pre-ran native gel (6% acrylamide

59:1, 0.25xTBE pH 8.3, 2.5% glycerol) and subjected to 160 V, 10 mA electrophoresis. After drying the gel was exposed on a Phosphoimager Screen (Amersham Biosciences) (3 h@rt) and scanned by a Typhoon 9400 scanner (Amersham Biosciences; Image Quant 5.0 Software). Densitometry was performed using ImageQuant TL (Amersham Biosciences). The affinity constants (K_D values) were extracted as mean values from 500× molar competition assays using a limiting amount of probe (5×10^{-10} M) and the protocol of Carey and Smale (2000).

Coimmunoprecipitation of proteins from crude embryonic extracts

Preparation of *Drosophila* crude embryonic nuclear extracts was performed from large scale embryo collections (~3–5 g), after Sullivan et al. (2000), apart from the following modification: nuclear proteins were extracted in (15 mM Hepes pH 7.9, 100 mM KCl, 50 mM NaCl, 0.1 mM EDTA, 0.1 mM EGTA, 1.5 mM MgCl2, 1 mM DTT, 1 mM PMSF) (1 ml/ g nuclei) for 45 min with gentle shaking on ice. 1.5 mg of crude nuclear extract was used in the IP including 50 μg of mouse-anti-Col (gift from Alain Vincent, Toulouse) in a volume dilution 1:100, or 35 μg of polyclonal rabbit-anti-GST-CncA (gift from Williams McGinnis, UCSD) in a volume dilution 1:900. Same amount and same dilution of mouse-anti-BP102 or rabbit-anti-bgal was used in the mock IP. The final volume of the IP reaction was adjusted with IP buffer (25 mM Hepes pH 7.9, 10 mM Tris pH 8.0, 1 mM DTT, 1 mM PMSF, 150 mM NaCl). The remaining of the assay was carried out after Wodarz (2008).

In vitro coimmunoprecipitation

The HA tag [YPYDVPDYA] N-terminal fusion of CncB was isolated by PCR using HA_Forward and CncB_Reverse primer from pRActHAdh (HAN_CncB) (Ntini and Wimmer, unpublished results), and cloned in the SmaI site of pTNT (Promega). HAN-CncB, ColA and ColB were expressed *in vitro* as described above. 12 μl of TNT reactions were mixed and incubated for 30 min at room temperature in 1x Binding Buffer. Then 2 μg of rabbit-anti-HA (Y-11 sc805, Santa Cruz Biotechnology Inc.) or rabbit-anti-bgal were added, the reactions were adjusted to the IP buffer concentrations (25 mM Hepes pH 7.9, 10 mM Tris pH 8.0, 1 mM DTT, 1 mM PMSF, 150 mM NaCl) in a final volume of 100 μl and incubated overnight at 4 °C with gentle shaking. The remaining of the assay was carried out after Wodarz (2008).

Fluorescent immunostaining

Methanol-stored fixed embryos were gradually rehydrated in PBX (PBS, 0.1%Triton-X). Blocking was in BBX (PBX, 0.1% BSA) supplemented with 20% Western blocking reagent (Roche) (1 h@rt). Primary antibodies were added in BBX; mouse-a-Col was applied at 1:50 dilution and rabbit-a-Cnc at 1:300 (overnight at 4 °C). Secondary antibodies (Alexa 488 a-mouse, Cy3 a-rabbit) were added at 1:300 (1.5 h@rt). Nuclear staining was with Hoechst 33342 at 1:1000 in PBX.

Microscopy

Embryos stained after *in situ* hybridization were mounted in glycerol (~90%) and documented with a Zeiss Axioplan 2 microscope (20× or 40× planes) using the ImageProPlus software (Version 6.2; MediaCybernetics). Pictures of fluorescent immunostained embryos (single planes or merged stacks) were taken with a Zeiss LSM 510 as previously described (Mavrakis et al., 2008; Smith, 2001). Embryonic staging was after Campos-Ortega and Hartenstein (1997).

In silico analysis of DNA sequences

In silico analysis to identify putative recognition sites within *cis*-regulatory regions was performed using MatInspector (MatInspector: Search for transcription factor binding sites http://www.genomatix.de/online_help/help_matinspector/matinspector_help.html; http://www.genomatix.de/cgi-bin/matinspector_prof/mat_fam.pl), the rVISTA browser (http://genome.lbl.gov/vista/rvista/submit.shtml) and position weight matrices (PWMs) of transcription factors annotated in the TransFac Database (http://www.biobase-international.com/index.php?id=transfac). Predictions were inspected manually, checked in correlation with literature reports and filtered through phylogenetic conservation using the *Drosophila* EvoPrinter (http://evoprinter.ninds.nih.gov/evoprintprogramHD/evphd.html) or the *Drosophila* UCSC Genome Browser (http://genome.ucsc.edu/cgi-bin/hgGateway). Genome-wide scan analysis was performed using the Genome Enhancer 2.0 (http://opengenomics.org/). Prediction of NLS was performed using the PredictNLS server (http://cubic.bioc.columbia.edu/services/predictNLS/) (Cokol et al., 2000) and prediction of SUMOylation motifs was performed using the SUMOsp 2.0 server (http://sumosp.biocuckoo.org/prediction.php) (Ren et al., 2009).

Plasmids for transient transfection and reporter assays

The sequence of *Dm_hh* promoter (−120 to +99 bp) was initially isolated with primers CAACGCGGAATGAACTCGAGGCGATAG (XhoI_-Forward) and AACTAGTTAGCTCTCGGTTCGGACAACCGTTG (SpeI_Reverse) and subcloned in XhoI/HindIII (T4 blunt) of pGL3-Basic Vector (Promega) which encodes firefly luciferase activity. Double-stranded oligos of the Collier DNA-binding site (5′ CGGCAGCAATTCCCCAATGGCATTTCACTT 3′) and the sequence which bears point mutation in the core (5′ CGGCAGCAAT**GAA**CCAATGGCATTTCACTT 3′) were ligated blunt in the SmaI site of the pGL3-*hh* promoter vector. Open reading frames of ColA and ColB were proofreading amplified with primers XhColF (CACCCTCGAGCTGGGCATGGAGTG)/SallColARev (GGTCGACTTATTTGGTTGACGTCACCAGTTG) and XhColF/XhoIColBRev (CCTCGAGTTAAACGGCCGCCGCCGTGGCTG), respectively. The clone 'ColA (1–534)' which encodes for a C-terminal truncated form of ColA lacking the last 23 amino acids was a sequenced clone obtained during cloning procedures. 'ColA RK' and 'ColB RK' clones (the K residue of the SUMOylation motif is mutated to R) were obtained by PCR-mediated point mutagenesis using the overlapping internal mutating primers colRK_F (CGATGACCTCGCTGAGGGAGGAGCC) and colRK_R (GGCTCCTCCCTCAGCGAGGTCATCG). DNA sequences of the open reading frames were subcloned in the SalI site of the RActHAdh vector under the control of the constitutive *act5C* promoter and *Adh* polyadenylation signal (Swevers et al., 1996). For luciferase reporter assays, S2 R+ cells were seeded into 12-well plates in Schneider's medium at 180,000 cells/ well. Next day, cells were cotransfected with 2 μg of total DNA (200 ng pRL (Renilla), 400 ng of Luciferase reporter plasmid, 800 ng of effector protein plasmid, 600 ng of empty RActHAdh vector) and 4 μl of Turbofect (Fermentas) according to standard protocol (Fermentas). After 48 h cells were lysed and Renilla-normalized reporter assays were performed using the Dual-Luciferase Reporter Kit (Promega). Activities were read in a 96-well format using a Berthold Centro LB 960 plate reader. Every experiment using cell culture was repeated at least twice, with two or more replicates within each independent experiment. Fold activation (Fig. 2B) is the ratio of Renilla-normalized reporter activation by the effector protein to that of the empty RActHAdh vector (1.4 μg of empty RActHAdh vector cotransfected with 200 ng pRL and 400 ng reporter plasmid). Error bars represent the positive standard deviation of at least two technical replicates in a representative experiment. Statistics was performed with Student's t-Test (two-tailed, unequal variance) using Microsoft Excel software.

Construction of deletion mutant reporter plasmids

Deletion mutant constructs lacking highly conserved sequence blocks in the context of the minimum 335 bp *ic-CRE* (Figs. S2, S3) were prepared in two-step cloning; 3′ part of the *ic-CRE* was amplified

using primers NruI_Forward (mutF1–mutF6) (Fig. S3) and XhoI_*hhR4* (Reverse) and subcloned into *pSLaf[Dm_hh promoter_tgfp_SV40]* (Ntini and Wimmer, 2011). 5′ part of the *ic-CRE* was amplified with primers BglIIF5 (Forward) and NruI_Reverse (mutR1–mutR5) (Fig. S3) and subcloned in the vector containing the respective 3′ part. Schematically the procedure is depicted in Fig. S3. The sequences of the primers are available upon request.

Site-directed PCR-mediated point mutagenesis

Constructs bearing point mutations in highly conserved blocks in the context of the 450 bp *ic-CRE* sequence (−3914 to −3465 bp) were generated by overlapping PCR site-directed point mutagenesis. Overlapping forward and reverse primers were designed bearing point mutations affecting targeted nucleotide positions. In order to insert the point mutation in the Collier binding site, the 5′ and 3′ fragments were amplified with primers [BglIIγ1mF5_colsitemutR (GAAATGCCATTGG**TTC**ATTGCTGCCGAAATAG)] and [colsitemutF (CTATTTCGGCAGCAAT**GAA**CCAATGGCATTTC)_hhR4] respectively, in separate proofreading (Pfu polymerase, Fermantas) PCR reactions using minimum amount of plasmid DNA template (~10 ng). PCR product bands were excised from agarose gel, DNA was purified (QIAGEN) and eluted in 20 μl of TE pH 8.5. 2–3 μl of each elution of the corresponding 5′ and 3′ products were combined in a final 50 μl proofreading PCR reaction; after an initial round of denaturation and annealing (so that the overlapping 3′ and 5′ sequences of the fragments hybridize and function as primers for the next elongation round) the 450 bp *ic-CRE* sequence was amplified with the external primers BglIIγ1mF5_hhR4 (sequences are available upon request). Fragments were then subcloned in *pSLaf[Dm_hh promoter_tgfp_SV40]* (Ntini and Wimmer, 2011) to generate the respective '450 bp *ic-CRE*_point mutation' reporter constructs. These were then assayed at the same genomic integration site [*attP 96E*; Bischof et al., 2007].

Generation of a Collier B-specific RNA probe for whole mount embryo in situ hybridization

The ColA and ColB cDNAs differ from each other by 465 nucleotides which are the result of a developmentally regulated splicing event (Crozatier et al., 1996). The 465 bp sequence, which is intronic for Collier A while coding for Collier B, was amplified with primers ColB_specific_F (TGTCCGCCGTGTCGTCGACGTG) and ColB_specific_Rev (CGTTAATCGTGTGTTGTCTGTGGTGTTTTG). The fragment was cloned in the PCRII vector (Invitrogen) and was used as a template to generate a Dig-labeled antisense RNA probe that specifically hybridizes with transcripts of Collier B in *in situ* whole-mount embryonic hybridization. Cytoplasmic transcripts detected with this probe are only of ColB while detectable nuclear dots correspond to total nascent transcripts (nuclear-dot staining is not distinguishable between ColA and ColB cell-group-specific expression).

Drosophila strains

Drosophila mutant alleles used were col^{1} (16), cnc^{VL110} (Mohler et al., 1995). Ectopic expression of *collier* and *cncB* was achieved using the lines *UAS-kn.M* (encodes *UAS-Collier B*; 45) and *UAS-CncB* (Veraksa et al., 2000), respectively, driven in an anterior embryonic gradient under the control of anterior localized maternal driver *pnos-GAL4/GCN4-bcd 3′ UTR* (Janody et al., 2000). The open reading frame of the Collier A isoform was cloned into the pUAST vector (Brand and Perrimon, 1993) (EcoRI) to generate pUAS-ColA. Two novel *UAS-Collier A* lines (on the second and on the third chromosome) were generated via *P*-element transgenesis. To generate a heat-shock inducible transgenic RNAi line of *collier*, the coding sequence of Collier A was cloned in antisense orientation into the EcoRI site of *pSLafHSaf* (Ramos et al., 2006) to generate *pSLaf_HS.ColA antisense_af*. The cassette consisting of {*heat-shock promoter_ColA_antisense_heat-shock 3′ UTR*} was excised with AscI and subcloned in the *pBac_attB* vector (Ntini and Wimmer, 2011). The resulting construct was injected in the *attP-96E* combined line (Bischof et al., 2007) to generate transgenic line HS.ColA_antisense #M3. Males transgenic for the *ic-CRE* 450 bp, homozygous on the third chromosome were crossed to virgins of *HS.ColA_antisense/TM2*. For heat-shock inducible transgenic RNAi of *col*, embryos of this crossing were collected for 1.5 h at room temperature, let to develop for 2.5 h, heat-shocked for 30-45 min at 37 °C and then let to develop at room temperature (22 °C) for 6–8 h before dechorionization (for 5–6 min) and fixation. *The UAS-slp1* hairpin line (Transformant ID 15749) was obtained from the VDRC Stock Centre, Vienna (Dietzl et al., 2007).

Results and discussion

Transcription factor binding sites within the hedgehog intercalary-specific cis-regulatory element

In the context of an analysis to identify *cis*-regulatory elements controlling expression of segment polarity genes in the embryonic head, an intercalary-specific *cis*-regulatory element of *hh—ic-CRE*—was isolated within the upstream 6.43 kb region (Ntini and Wimmer, 2011). The ~1 kb enhancer fragment (−4085 to −3077 bp) mediates reporter expression in the *hh* expressing cells of the posterior part of the intercalary segment, when combined with the endogenous *hh* promoter (−120 to +99 bp; Fig. S1B). Further functional dissection of this element (Fig. S1A) showed that the 450 bp *γ1mF5* subfragment (−3914 to −3465 bp) mediates the intercalary-specific expression (Fig. 1A) with slightly delayed onset, while the 335 bp *F5_R4* subfragment (−3799 to −3465 bp) constitutes the minimum sequence required for the intercalary expression, but mediates an additional spotty metameric pattern in the trunk (Ntini and Wimmer, 2011). Because a high degree of phylogenetic conservation in non-coding DNA sequence implicates a functional role *in vivo*, such as recognition and DNA-binding by sequence-specific transcription factors (Bejerano et al., 2005), the sequence of the *ic-CRE* was subjected to phylogenetic conservation analysis within the genome of twelve *Drosophila* species, and different *in silico* analyses (Material and Methods) were performed to detect putative transcription factor binding sites. The minimum 335 bp *ic-CRE* consists of six highly conserved sequence blocks (I–VI; Fig. S2). A series of complete block deletions designed in the context of the minimum *ic-CRE* in combination with the endogenous *hh* promoter resulted in non-functional elements (Fig. S3). This could be either because individual binding motifs were disrupted or inter-motif distances crucial for transcription factor binding and operation were disturbed. We then conducted a point mutagenesis screen in the context of the 450 bp *ic-CRE* to extract crucial *cis*-regulatory information in respect to the conserved *in silico* identified transcription factor binding sites (Fig. S1A).

The *ic-CRE* responds to the homeotic transformation of the mandibular into an intercalary segment resulting from ectopic *ems* expression (Schöck et al., 2000) by a duplication of its expression pattern (data not shown). However, despite this and the fact that the *Hox* gene *labial* is active in the intercalary segment (Diederich et al., 1989; Merrill et al., 1989), disrupting the homeodomain binding sites in conserved sequence blocks III or IV (Fig. S1A) by point mutations did not abolish the *ic-CRE* mediated reporter expression (Fig. 1C). In contrast, disrupting a putative binding site for the fork head transcription factor Sloppy paired 1 (Slp1) in block IV (Fig. S1A) eliminated the *ic-CRE*-mediated reporter expression (data not shown). This is consistent with the reduced reporter expression in an RNAi-mediated knock-down of *slp1* (Fig. 1D), which is a proposed head gap-like and pair rule segmentation gene (Grossniklaus et al., 1994).

In silico predicted COE DNA-binding site within the ic-CRE is functionally required

Another *in silico* prediction was found in conserved block II at position −3771 to −3755 bp (Fig. S1A) that scores the binding matrix

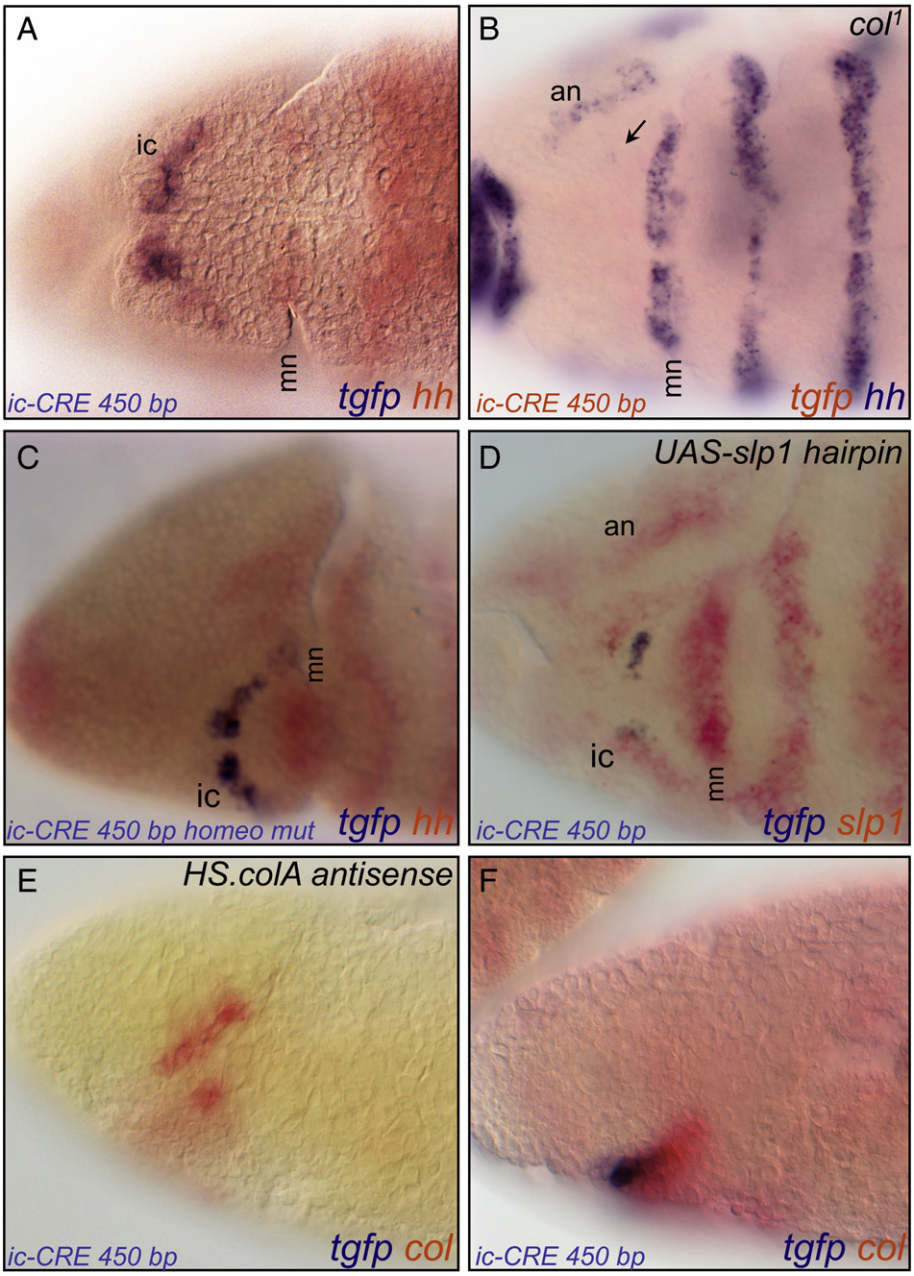

Fig. 1. Pattern of the *ic-CRE* mediated reporter expression in various genetic backgrounds, analyzed by whole mount embryo *in situ* hybridization. (A) Red staining (FastRed) marks the endogenous *hh* expression, blue staining (NBT/BCIP) marks the mediated *tgfp* reporter expression. The 450 bp *ic-CRE* sequence (−3914 to −3465 bp) mediates reporter expression in the cells of the posterior part of the intercalary (ic) segment overlapping the endogenous intercalary *hh* expression. (B) The *ic-CRE* mediated expression and the intercalary *hh* expression are abolished in *collier* loss-of-function background (*col*^{1}; Crozatier et al., 1999). The arrow marks the intercalary segment. The other segments are marked by *hh* expression (NBT/BCIP; blue staining). (C) Disrupting by point mutation the putative homeodomain recognition sites of the third conservation block (Fig. S1A) in the context of the 450 bp *ic-CRE* sequence does not affect the mediated reporter expression pattern. (D) The *ic-CRE*-mediated expression is greatly reduced in an RNAi-mediated *slp1* knock-down background created by crossing the *UAS-slp1* hairpin (VDRC #15749; Dietzl et al., 2007) to *pnos_GAL4/GCN4_bcd 3′ utr*. Weak red staining marks remnants of *slp1* transcripts after knocking-down *slp1* expression by RNAi. (E) The *ic-CRE* mediated expression is abolished in a transgenic antisense-mediated *col* knock-down, for which a newly generated *HS.ColA_antisense* line was used (#M3). Weak red staining marks remnants of *col* sense transcription after knock-down by heat-shock induced *col* antisense transcription. (F) A transgenic heat-shocked embryo that does not bear the *HS.ColA_antisense* insertion.

(Fig. S1C) of the mammalian COE factor Olf1 (Wang et al., 1993). Disrupting this site by point-mutation resulted in the complete abolishment of the *ic-CRE* mediated reporter expression (data not shown), indicating that the site is absolutely required for the function of the 450 bp *ic-CRE* (Fig. S1A). Olf1 is the mammalian COE homolog of Collier and the endogenous *hh* expression in the intercalary segment is abolished in a *col* loss-of-function mutant (*col*^{1}; Crozatier et al., 1999). Likewise, the *ic-CRE*-mediated expression pattern is abolished in *col*^{1} or *col* knock-down (Figs. 1B, E, F). In addition, the DNA-binding domain of Collier displays a high degree of primary sequence identity (86%) to the mammalian homolog (Crozatier et al., 1996). High degree of primary sequence identity in the DNA-binding domain, shared among the members of the COE family allows for a similar DNA-binding specificity: both Collier and the *Xenopus* homologs recognize the mammalian DNA target sequences *in vitro* (Daburon et al., 2008; Pozzoli et al., 2001). Therefore, we regarded the Olf1 prediction

identified *in silico* within the *ic-CRE* as a putative Collier binding site and refer to this as a Collier recognition site.

Apart from this functionally required Collier recognition site at -3773 to −3751 bp, scanning *in silico* the 6.43 kb upstream *hh* enhancer using MatInspector (Cartharius et al., 2005) with a similarity cut-off of 1, 0.8 (core, matrix) identifies one more Olf1 prediction within the *ic-CRE* at position −3967 to −3945 bp (Fig. S4). The 6.43 kb upstream enhancer of *hh* was also submitted to rVISTA (Loots et al., 2002) using the nucleotide positions 3–19 of the binding matrix of Olf1 (Fig. S1C). When setting the highest possible similarity cut-off 0.95, 0.85 (core, matrix), so that at least one prediction is generated, then only the functionally required Collier recognition site CAATTCCCCAATGGCAT (at −3771 to −3755) within the *ic-CRE* is detected. Lowering the matrix similarity threshold by 0.05, using cut-off 0.95, 0.8, generates three additional predictions. These are two distant sites, GAGACACTTGGGATGAG at −3963 to −3947 and CACACCACGGGGAAGCG at −2872 to −2856, and one promoter-proximal site CACTTCCCTTGCGCATA at −212 to −196 (Fig. S4). The first distant site is within the *ic-CRE*, 190 bp upstream of the functionally required Collier recognition site, and is also predicted by the MatInspector. Interestingly, in contrast to the functionally required Collier recognition site within the *ic-CRE*, none of the other predicted sites are phylogenetically conserved among the twelve *Drosophila* species. Considering the displayed short-range homotypic clustering (within 200 bp; Fig. S4), it is, however, possible that the weaker predictions may contribute to the transcriptional outcome (Segal et al., 2008) of the *ic-CRE*, even though they might be recognized with minor affinity by Collier *in vivo*.

Occupancy of the functionally required Collier recognition sequence in vivo

In order to verify that the *in silico* identified and functionally required Collier recognition site within the *ic-CRE* is indeed occupied by Collier *in vivo*, we performed chromatin immunoprecipitations (ChIP) from *Drosophila* embryonic nuclear extracts with an antibody against Collier (gift from Michele Crozatier and Alain Vincent). In the anti-Col ChIPs, the functionally required Collier binding site within the *ic-CRE* was specifically enriched in comparison to mock ChIPs (Fig. 2A), which indicates that the site is indeed occupied by Collier *in vivo*.

Both isoforms encoded by collier/knot possess transcriptional activation potential

In the case of the mammalian COE homolog of Collier, it was previously deciphered that the mouse transcription factor EBF contains two distinct and functionally independent transcription activation domains, the second one within the C-terminal region (Hagman et al., 1995). Although *Drosophila* Collier has been genetically implicated as an activator of downstream segment polarity gene expression (Crozatier et al., 1999), its transcriptional activation potential had not yet been analyzed. In *Drosophila* two Collier isoforms are expressed from the *col* gene locus. The cDNAs encoding Collier A (also termed Col2) and Collier B (Col1) differ from each other by 465 bp due to alternative splicing (Crozatier et al., 1996). The two protein isoforms share the same first 528 N-terminal amino acids and differ in the C-terminal 29 amino acids for Collier A and 47 amino acids for Collier B. No specific expression pattern of *collier A* could be detected by double *in situ* hybridization using an RNA probe specific for *collier B* and a probe that hybridizes with both transcripts (Materials and methods).

Therefore the transcriptional activation potential of each of the two Collier isoforms was examined by reporter assays in *Drosophila* S2 R+ cell transfections. In the reporter construct the functionally required and *in vivo* occupied Collier site (CGGCAGCAATTCCCCAATGGCATTTCACTT) was cloned in a single copy upstream of the endogenous *hh* promoter (−120 to +99 bp) driving *luciferase* gene expression. Both Collier isoforms activate luciferase expression when independently co-transfected with the reporter construct (Fig. 2B), indicating that both isoforms possess transcriptional activation potential. A truncated form of ColA lacking the last 23 C-terminal amino acids (ColA 1–534) displays a significantly reduced activation potential (~84% decrease, $P<0.001$), which indicates that a transcriptional activation domain must reside within either C-terminal region of both isoforms. Disrupting the Collier recognition site by point mutations (CGGCAGCAAT**GAA**CCAATGGCATTTCACTT) decreased the mediated reporter activation by ~48% in the case of Collier A ($P<0.01$) and ~44% in the case of Collier B ($P<0.05$). Taking into consideration that disrupting the Collier binding site in the context of the *ic-CRE* (Fig. S1A) resulted in a complete abolishment of the mediated reporter expression *in vivo*, and that the same mutation does not support Collier DNA-binding *in vitro* (see below; Fig. 3B), we assume that part of the reporter activation assessed in cell transfection may be achieved by Collier transactivating via unknown system-provided DNA-binding activities on the regulatory sequences of the reporter plasmid (as mentioned above, it includes the endogenous *hh* promoter sequence −120 to +199 bp). Moreover, Collier carries a perfect SUMOylation motif within the N-terminus, predicted with the highest threshold value (Ren et al., 2009). The protein sequence TSLKEEP at amino acid position 44-50 matches the SUMOylation motif Ψ–K–X–E (Ψ, a hydrophobic amino acid). Additional members of the COE transcription factor family contain also a SUMOylation motif at this conserved position (Daburon et al., 2008). Apart from antagonizing ubiquitin-mediated degradation, sumoylation has been implicated in modifying transcriptional activation/repression potential of transcription factors (reviewed in Zhao, 2007). Mutant versions of Collier A and Collier B where the K within the SUMOylation motif is mutated towards R (ColA RK and ColB RK) display reduced activation potential ($P<0.05$ and $P<0.01$, respectively), implying a possible role for sumoylation in regulation of Collier transcriptional activity (Fig. 2B).

In vitro analysis of Collier DNA-binding to the functionally required COE site of the ic-CRE

Next we examined in electrophoretic mobility shift assays (EMSA) the ability of the two Collier splicing isoforms to bind *in vitro* the functionally required recognition site, primarily identified *in silico* within the *ic-CRE*, and occupied by Collier *in vivo*. Apart from the 'wild type' sequence, an optimal sequence bearing two nucleotide exchanges to perfectly match the binding matrix of Olf1 (Fig. S1C) was also assayed as a binding probe. Both sequences were bound by the two isoforms leading to the formation of a major shift complex (C1; Fig. 3A). According to previous studies (Daburon et al., 2008) and since dimerization of the COE family members is mediated by the HLH domain (Daburon et al., 2008 and references therein), C1 is formed due to homodimer and/or heterodimer binding when both factors are included in the reaction. The two isoforms differ only slightly in their molecular weight, thus migration of the heterodimer state is not separable from either homodimer. Only in the case of Collier B one additional faster migrating complex (C2; Fig. 3A) is detected which is most probably due to Collier B binding also as a monomer. Modest monomer DNA-binding activity has been reported in the case of the mammalian COE homolog EBF as well (Hagman et al., 1995).

Specificity of the detected Collier DNA-binding complexes was resolved in competition assays using as cold oligo competitors mutant versions of the wild-type sequence bearing nucleotide exchanges (Fig. S1C). In contrast to the wild-type oligo that causes a detectable competition effect at 100x molar excess (lanes 2, 8, Fig. 3B), a competitor bearing point mutations in a position corresponding to the core of the binding matrix of the mammalian homolog (competitor mut2; Fig. S1C) is not recognized by Collier, thus incapable of competition at the same molar excess (lanes 4, 10, Fig. 3B). A competitor bearing point mutations 5' of the core (competitor mut1) competes but not as efficiently as the wild-type version (lanes 3, 9, Fig. 3B).

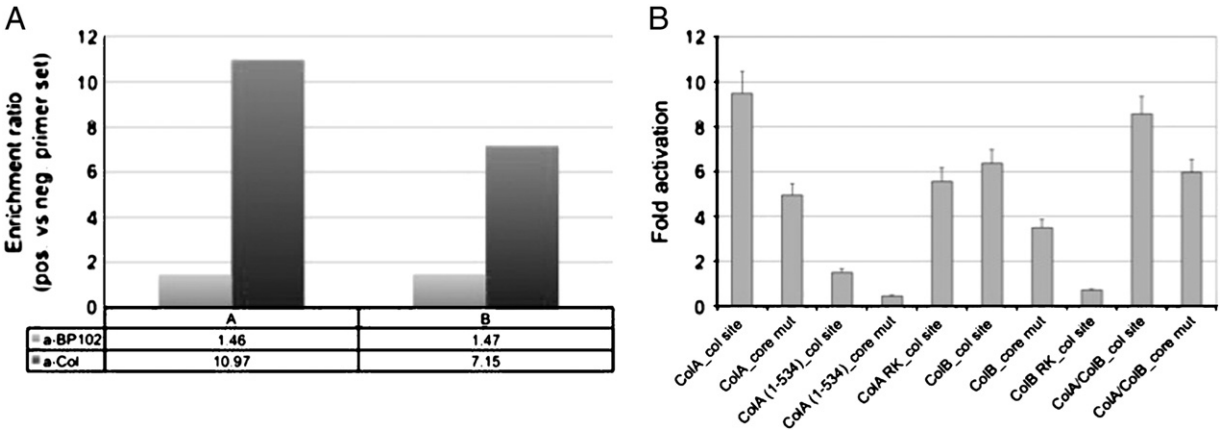

Fig. 2. *In vivo* occupancy of the functionally required Collier DNA-binding site and activation potential of Collier isoforms. (A) *In vivo* occupancy of the Collier recognition site within the *ic-CRE* (Fig. S1A) assayed by ChIP from embryonic nuclear extracts. The site is specifically enriched in the anti-Col IP samples in comparison to the mock IP's. Enrichment of the target sequence of the Collier binding site was assessed by qPCR and it is expressed as a ratio over a negative control region. The latter is an amplicon within the second exon of *caudal*. A, B are two biological replicates starting from independently isolated embryonic extracts. (B) The wild type sequence of the Collier DNA-binding site CGGCAGCAATTCCC-CAATGGCATTTCACTT ('col site') or the site bearing point mutations CGGCAGCAAT**GAA**CCAATGGCATTTCACTT ('core mut') were cloned upstream of the endogenous *hh* promoter (−120 to +99 bp) driving luciferase gene activity to assay transcriptional potential of Collier factors in S2 R+ cell transfection. Both Collier isoforms possess transcriptional activation potential. ColA(1–534) is a truncated form depleted of the last 23 C-terminal amino acids. ColA RK and ColB RK bear the (K>R) mutation in the SUMOylation motif.

This result indicates that the altered nucleotides are also contacted by Collier, thus contributing to the stability of the detected DNA–protein interaction *in vitro*. Competition affects likewise formation of the C2 complex of Collier B (lanes 7–12, Fig. 3B) indicating that specific DNA–protein interactions by monomers of Collier B can form *in vitro*. The sequence of the competitor oligo 3 (lanes 5, 11, Fig. 3B) is found within the *ic-CRE* at position −3674 to −3650 bp and, although not phylogenetically conserved, it was picked for competition

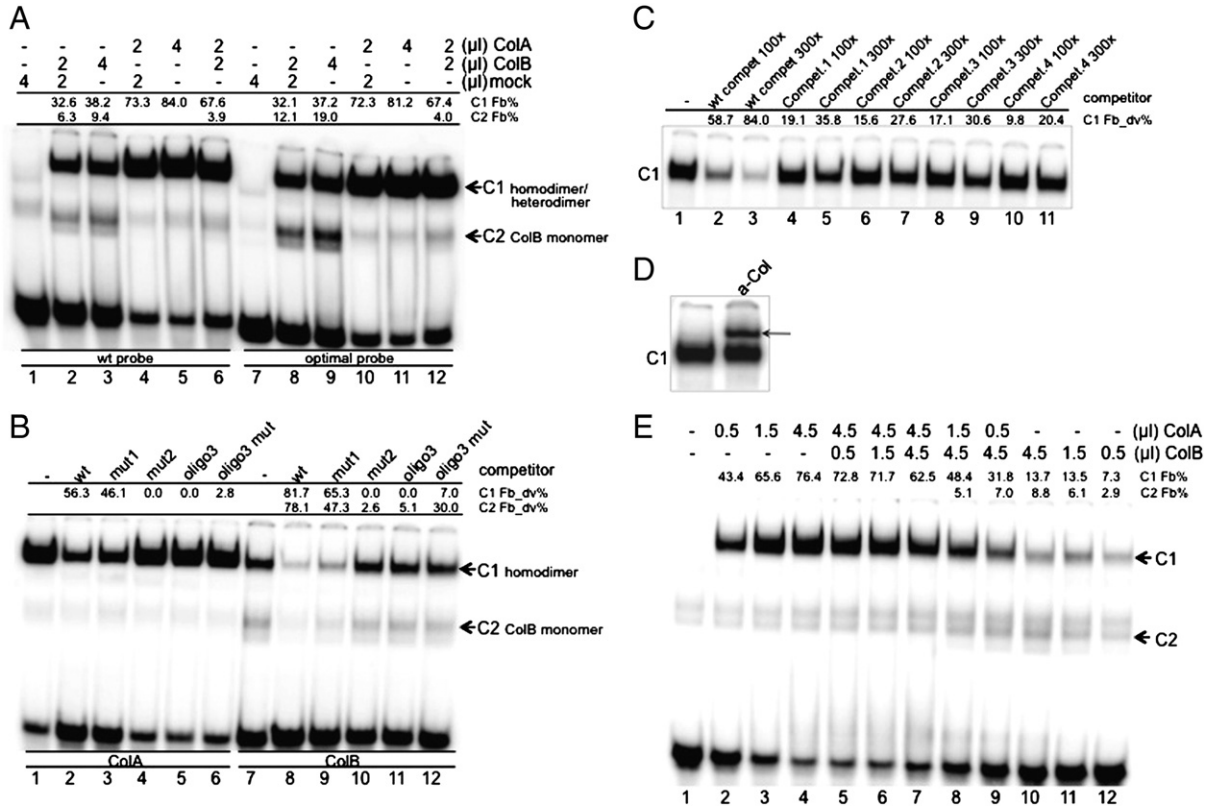

Fig. 3. *In vitro* analysis of Collier DNA-binding to the functionally required COE site of the *ic-CRE*. (A) Mobility shift assay of the two Collier isoforms A and B with the wild type (lanes 1–6) or optimal sequence (lanes 7–12) probe. The sequences of the probes are found in Fig. S1C. C1 complex is due to Collier A (lanes 4, 5, 10, 11) or Collier B (lanes 2, 3, 8, 9) homodimer DNA-binding, and/or heterodimer DNA-binding when both factors are included in the binding reaction (lanes 6, 12). C2 is due to Collier B monomer DNA-binding. (Fb%, bound fraction of DNA). (B) Competition assay with different cold oligo competitors at 100x molar excess. Fb_dv % are % diminishment values in complex formation. The sequences of the different cold oligo competitors are found in Fig. S1C. (C) Competition assay at 100x and 300x molar excess: oligo competitors are *in silico* predictions of a lower matrix similarity cut-off (0.8; Competitor 1–3) within the 6.43 kb upstream *hh* enhancer (Fig. S1C, S4). Both Collier isoforms are included in formation of C1. (D) The arrow depicts the supershift band produced in the presence of anti-Col antibody (both Collier isoforms included in C1 formation). (E) Titration assay of the two Collier isoforms with the wild type sequence probe. In lane 1, 9 µl of mock TnT reaction are included. In all reactions the total protein volume is adjusted to 9 µl by adding the corresponding volume of mock TnT reaction. Adding increasing amount of ColB to constant ColA leads to decrease in C1 complex formation (lanes 4–7). Adding increasing amount of ColA to constant Col B leads to decrease in C2 while C1 increases (lanes 10–7).

since it bears the four nucleotides — TCCC — corresponding to the core of the mammalian binding matrix. Neither this, nor a mutant version of it (oligo 3 mut; lanes 6, 12, Fig. 3B) compete.

Additional competition assays for CollierA/B DNA-binding complexes were carried out with the putative Collier recognition sequences predicted *in silico* within the −6.43 kb upstream region of *hh* (Figs. S4, S1C). These phylogenetically non-conserved sites and a sequence that scores the 5′ half of the Olf1 binding matrix (nucleotide positions 3–11), found also within the *ic-CRE* (at −3714 to −3706), were used as competitors in mobility shift assays with the probe encompassing the functionally required Collier binding site (−3771 to −3755) (Fig. 3C). All of the predictions assayed as cold oligo competitors produce a very weak competition effect (lanes 4–11) in comparison to the wild-type sequence of the functionally required Collier binding site (lanes 2, 3). This suggests that the functionally required Collier binding site of the *ic-CRE* is the major one within the 6.43 kb *hh* upstream region that is recognized and occupied by Collier *in vivo*.

By the use of an antibody against Collier (gift from Michele Crozatier and Alain Vincent) that produces a supershift in the EMSA (Fig. 3D), we could confirm both the presence of Collier in the C1 complex and the ability of the antibody to specifically recognize Collier in the DNA-binding conformation, which was an important prerequisite for the use of the anti-Col in the ChIP experiments (see above, Fig. 2A).

Collier B heterodimerizes with Collier A and the distinct dimerization states display differential DNA-binding affinities in vitro

In EMSA titration experiments, in which the amount of Collier B is kept constant, the addition of increasing amounts of Collier A leads to progressive increase in the dimeric C1 complex formation at the cost of Collier B monomeric C2 complex (Fig. 3E, lanes 10–7). In addition, when both factors are provided in equal amounts (Fig. 3E, lane 7), the DNA bound fraction of the C1 complex (Fb% 62.54) is not cumulative of the respective individual C1 values of the Collier A (Fb% 76.39, Fig. 3E, lane 4) and Collier B (Fb% 13.65, Fig. 3E, lane 10) homodimer–DNA complexes, but is instead less than the respective Collier A and greater than Collier B homodimer. When keeping the amount of Collier A steady at increasing amounts of Collier B, C1 complex formation decreases (Fig. 3E, lanes 4–7). The above data is indicative that in the presence of Collier A, Collier B molecules heterodimerize; Collier A and Collier B isoforms do not independently bind the oligo but rather heterodimerization and heterodimer DNA-binding occurs when both factors are present. Further, the affinity constant (K_D value) of the C1 complex was assessed in the case of the Collier A homodimer (16.80 ± 0.11 nM) and in the case when both factors are included in the reaction (37.16 ± 3.51 nM). We postulate that this difference in the K_D reflects heterodimerization between Collier A and Collier B and indicates that the heterodimer state binds the oligo with somewhat lower affinity than the Collier A homodimer. In the case of C1 homodimer complex formation by Collier B, the K_D was calculated higher (156.04 ± 48.68 nM) indicating even lower DNA-binding affinity *in vitro*. The *in vivo* biological relevance of the two Collier splicing isoforms to form heterodimer DNA-binding complexes remains to be explored.

Restriction of the activator function of Collier to the posterior part of the intercalary segment

In this study we provide evidence that Collier acts as a direct transcriptional activator of *hh* expression in the posterior part of the intercalary segment by occupying a newly identified DNA-binding sequence lying within the previously reported *ic-CRE* (Ntini and Wimmer, 2011). Nevertheless, *collier* expression is not restricted to the posterior part of the intercalary segment, but extends into the anterior part of the mandibular segment (Figs. 4 A, C, I) at the time when the intercalary *hh* expression is established. Only at a later stage, *col* expression gets restricted to the posterior part of intercalary segment (Figs. 4B, J, K; Crozatier et al., 1999). Therefore, a potential means of restricting the activating function of Collier to the cells of the posterior part of the intercalary segment was examined. This could be either the requirement for a co-activator absent from the cells of the anterior part of the mandibular segment or the presence of (a) repressive factor(s) in those cells. It was previously reported that the expression of *collier* overlaps the expression of *cap 'n' collar* (*cnc*) in the anterior part of the mandibular segment (Crozatier et al., 1999; Seecoomar et al., 2000; Veraksa et al., 2000). *cnc* encodes three bZIP isoforms of which only one (CncB) displays a key function in embryonic head development: *cncB* activity is required for the establishment of the mandibular segment identity (McGinnis et al., 1998; Veraksa et al., 2000) and its expression in the mandibular segment directly abuts the intercalary *hh* expression (Figs. 4D, E; 5A) as well as the *ic-CRE*-mediated reporter expression (Fig. 4G). We thus hypothesized that CncB might be involved in the repression of *hh* expression in the anterior most part of the mandibular segment where Collier and CncB are co-expressed (Fig. 4I) and examined this possibility.

Ectopic expression of CncB represses intercalary hh and ic-CRE-mediated expression

Ectopic expression of *cncB* in the complete embryonic head region using the anterior localized maternal driver *pnos_Gal4/Gcn4_bcd 3' utr* (Janody et al., 2000) causes modest to strong suppression of the endogenous *hh* expression (Fig. 5B) as well as repression of the *ic-CRE*-mediated reporter expression (Fig. 5C) in the cells of the posterior part of the intercalary segment. Expression of *hh* or the *ic-CRE* remains unaltered in a control genetic background where ectopic head expression of *lacZ* (not shown) or *col* (Figs. 5F, I) is generated using the same maternal driver. Ectopic expression of neither Collier A nor of Collier B, nor even the simultaneous ectopic expression of both Collier isoforms caused any change in *hh* or the *ic-CRE*-mediated expression. In these studies it is important to note, that neither the ectopic expression of *cnc* interferes with the endogenous expression of *col* (Fig. 5G), nor the ectopic expression of *col* changes the *cnc* expression (Fig. 5H). Thus CncB seems to act as a repressor of the intercalary-specific expression of *hh* mediated by the *ic-CRE*.

CncB activity is involved in late temporal down-regulation of intercalary-specific hh expression

Starting around stage 11, a gradual decrease in the intensity of the intercalary *hh* stripes, can be noticed (compare Fig. 4C with 5D). The process of turning-off procephalic segment polarity gene expression at late germ-band extension stages has been previously reported (Schmidt-Ott and Technau, 1992 and references therein). Interestingly, the fading of the intercalary ectodermal *hh* stripe is preceded by the secondary initiation of *cnc* expression in the *hh* expressing cells of the posterior part of the intercalary segment (Figs. 4F, H, J, L) which is actually triggered by *collier* activity (Crozatier et al., 1999). In *cnc* mutant embryos (cnc^{VL110}; Mohler et al., 1995), we observed irregular persistence of the intercalary *hh* expression (Fig. 5E). This is in concurrence with the proposed repressive function of CncB on the intercalary-specific transcriptional regulation of *hh*, even though we do not observe a posterior de-repression of the intercalary-specific expression of *hh* into the anterior part of the mandibular segment in *cnc* mutants, which might be due to redundant repressor activities.

CncB interferes with Collier DNA-binding activity in vitro

Within the *ic-CRE*, an imperfect match of the Cnc DNA-binding consensus (KTCAT; Veraksa et al., 2000) is found adjacent to the functionally required Collier binding site (Fig. S1A). However, Cnc

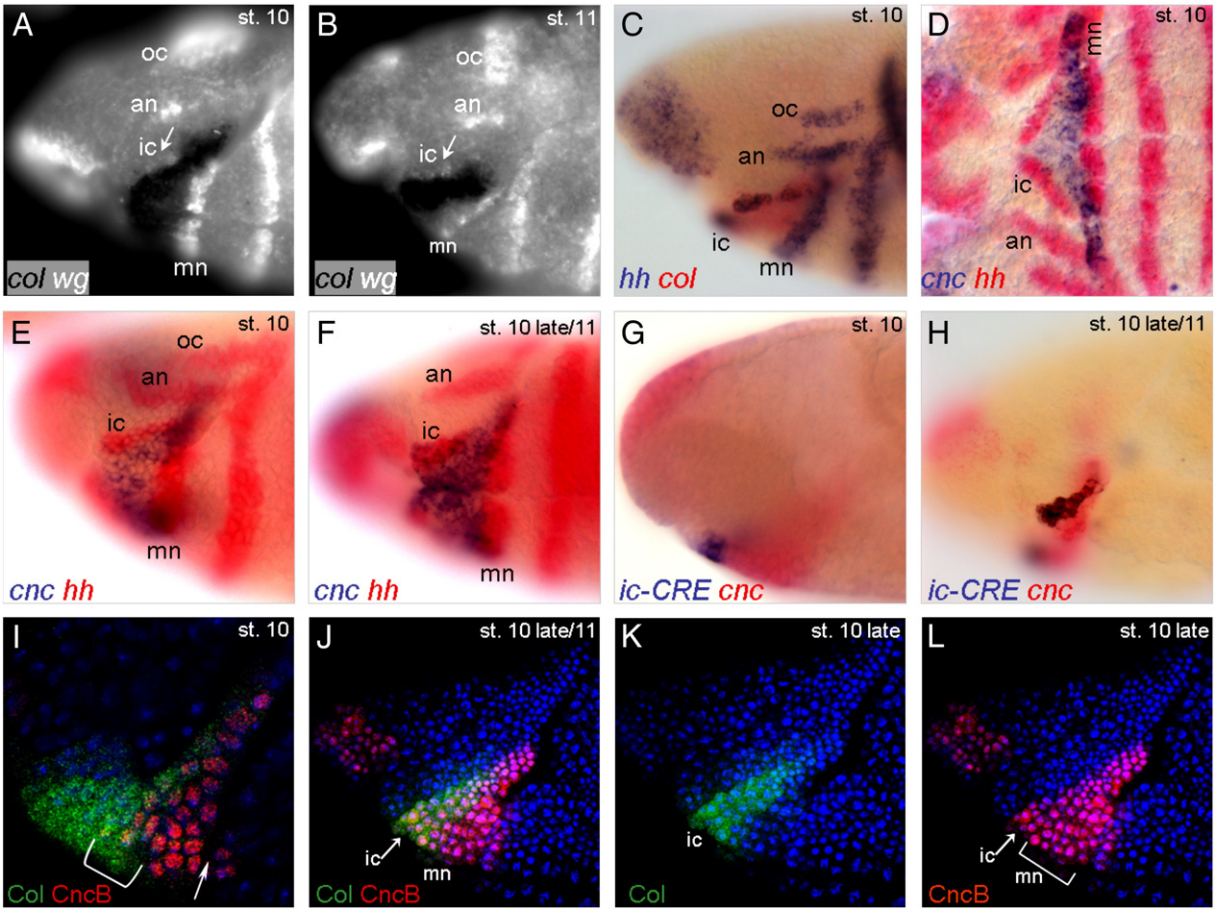

Fig. 4. Comparative expression patterns of the second order regulators Collier and CncB, in relation to the segment polarity genes *wg* and *hh* and the 450 bp *ic-CRE* mediated reporter expression pattern. (A–H) Double *in situ* hybridization (probes indicated at lower left corner of each panel). (I–L) Fluorescent immunostaining of Collier (Alexa 488, green) and CncB (Cy3, red). (A, B) The anterior border of *col* expression abuts the *wg* expressing cells of the intercalary segment depicted by the arrow. During germ band extension the posterior border of the *col* expression domain moves gradually towards the anterior (represented by the graded filling of the *col* bar in scheme of Fig. 5M). (C) During early stages of germ band extension (8–10) expression of *col* broadly overlaps the *hh* expressing cells of the posterior part of the intercalary segment exceeding also into the anterior part of the mandibular segment. (D, E) At stage 10, the early expression of *cnc* in the mandibular segment abuts the *hh* expressing cells of the posterior part of the intercalary segment and the *ic-CRE* mediated expression pattern (G). (F) During stage 10 a secondary initiation of *cnc* expression is triggered by *col* activity (Crozatier et al., 1999) in the posterior part of the intercalary segment. Then *cnc* overlaps the intercalary *hh* expressing cells and the *ic-CRE* mediated expression pattern (H). (I) Early restricted overlap of Collier and CncB expression in the cells of the anterior most part of the mandibular segment (bracket) detected at protein level. CncB has a major nuclear localization in contrast to the Collier activator. The arrow in I depicts ventrally the cephalic furrow. (J–L) Later on, Collier and CncB are coexpressed also in the—*hh* expressing—cells of the posterior part of the intercalary segment depicted by the arrow. The bracket in L marks the anterior part of the mandibular segment.

homologs (CncB or CncA) did not specifically bind the assayed probe *in vitro* (Fig. 5J and data not shown). This is in principle in agreement with Veraksa et al. (2000), who report that CncB achieves binding to its cognate site in the presence of the Maf-S (bZIP) cofactor that cooperatively binds to an adjacent recognition sequence. Nevertheless, when both Collier and CncB factors are included in the reaction, apart from the characterized Collier DNA-binding complex, no additional complex could be detected that would imply synergistic binding with Collier (Fig. 5J). On the contrary, addition of CncB to the Collier DNA-binding reaction leads to attenuation of Collier DNA-binding complex formation (Fig. 5J). This kind of sequestering effect of CncB on Collier DNA-binding activity is exerted in a dominant way: adding a constant amount of CncB to the Collier–DNA complex that has reached the binding equilibrium, leads to progressive 'stripping-off' of Collier protein molecules from the DNA-binding state when assayed for gradually longer incubation times prior to immediate gel loading (Fig. 5K). Thus, CncB functions as a dominant inhibitor of Collier DNA-binding activity *in vitro* and presumptively antagonizes the transcription activation potential of Collier *in vivo*. Such a kind of sequestering effect exerted by CncB on Collier DNA-binding activity requires a direct physical interaction between the two protein factors. Indeed, by using an antibody (gift from W. McGinnis, UCSD) that recognizes the CncB isoform (~90 kDa) on immunoblots of embryonic extracts, we could detect a major specific band in the anti-Col IP eluates from crude (not subjected to crosslinking) extracts, corresponding to the major band detected in the anti-Cnc IP eluate (Fig. S5). However, we were not able to reproduce the interaction *vice versa*, i.e. detect Collier in the anti-Cnc IP eluate. Therefore, in order to verify that indeed a protein interaction between Collier and CncB takes place, we performed *in vitro* coIP using *in vitro* expressed Collier A, Collier B and an N-terminal HA-tagged version of CncB (HAN-CncB). By using anti-HA, we could coimmunoprecipitate both Collier A and Collier B from [HAN-CncB/ColA] and [HAN-CncB/ColB] input, respectively (Fig. 5L).

Taken together, the *in vivo* as well as the *in vitro* data are consistent with CncB performing as a sequestering factor or inhibitor of Collier DNA-binding to its cognate site found within the *ic-CRE*. Furthermore, fluorescent immunostaining revealed that only a small fraction of the expressed Collier protein is nuclear localized *in vivo* (Figs. 4I, K). Conversely, CncB protein greatly accumulates in the nuclei (Figs. 4I–L). Prediction of nuclear localization signals (NLS) *in silico* (Cokol et al., 2000) generates no results for Collier, while CncB contains an NLS (RRRGKNKVAAQNCRKRK aa 622–638) within the bZIP domain (aa 617–680). Interestingly, Collier carries a perfect SUMOylation motif in

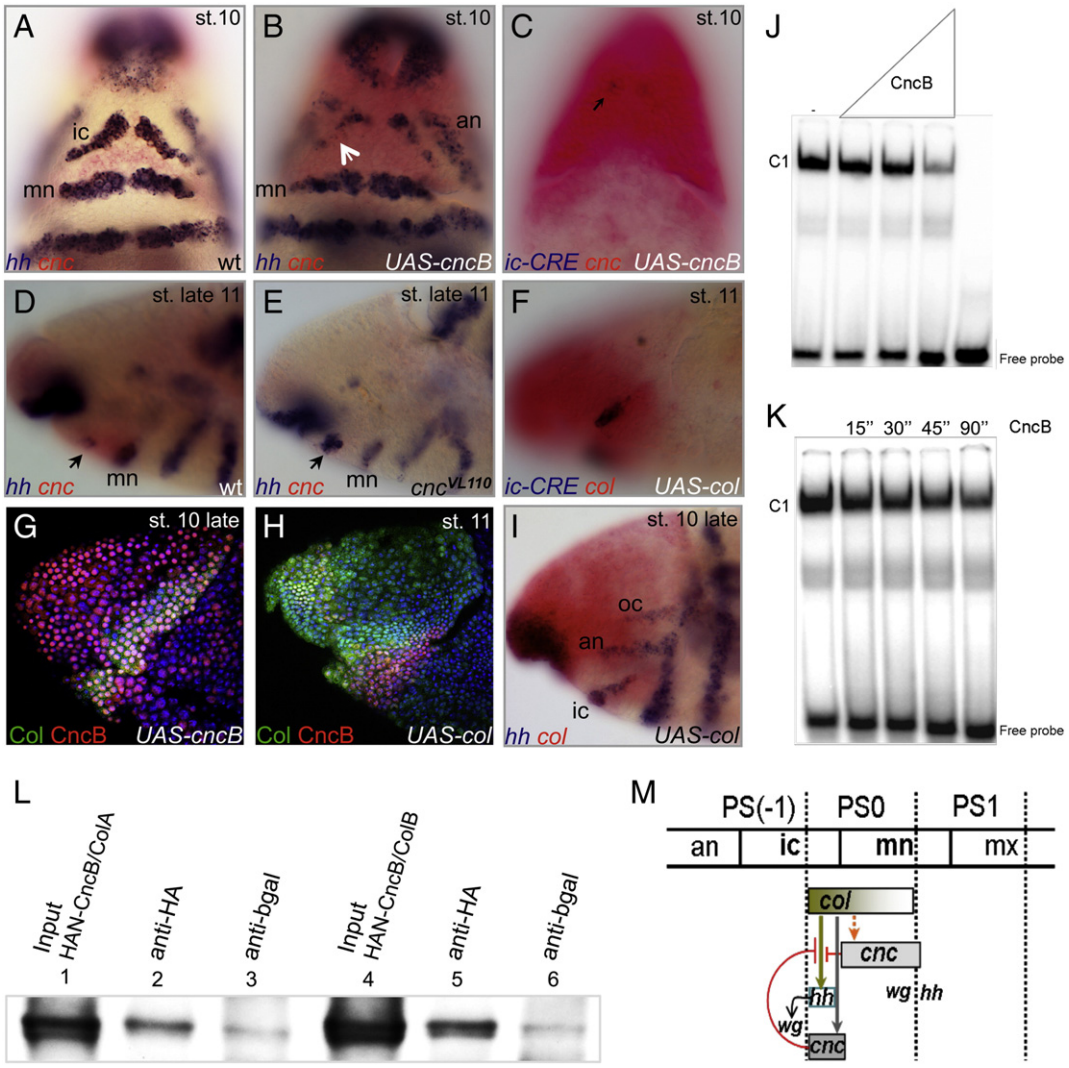

Fig. 5. Negative regulatory effect exerted by CncB on the intercalary-specific regulation of *hh* expression. (A–F, I) Double *in situ* hybridization (probes indicated at lower left corner of each panel). (G, H) Fluorescent immunostaining of Collier (Alexa 488, green) and CncB (Cy3, red). (A, B) Transcription of *hh* in the cells of the posterior part of the intercalary segment is partially suppressed when ectopic procephalic expression of *cncB* is driven early in development using the maternal driver *pnos_GAL4/GCN4_bcd 3′ UTR* (32). (**A**), wt; (B), *UAS_cncB/ pnos_GAL4/GCN4_bcd 3′ UTR* (progeny of the crossing between females homozygous for the driver on the second chromosome with males homozygous for *UAS-cncB* on the third chromosome). (C) The *ic-CRE* mediated expression pattern (arrow) is repressed in the same ectopically expressed CncB background. (D) Detection of the remaining intercalary *hh* transcription (arrow) in late stage 11 embryos of a wild type embryo. (E) Detection of the irregular persistence of *hh* transcripts in ectodermal cells of the intercalary lobes of late stage 11 cnc^{VL110} (44) null mutant embryos. (F) The *ic-CRE* mediated expression pattern is not altered in the ectopically expressed *col* background created using the *UAS-kn.M* (Mohler et al., 2000; encodes Collier B) under the control of *pnos_GAL4/GCN4_bcd 3′ UTR*. (G) Expression of Collier remains unaltered in ectopically expressed CncB under the control of *pnos_GAL4/GCN4_bcd 3′ UTR*. (H) Expression of CncB remains unaltered in ectopically expressed Collier (Collier A; using a newly generated *UAS-colA* line) under the control of *pnos_GAL4/GCN4_bcd 3′ UTR*. (I) Expression of *hh* remains unaltered in ectopically expressed *collier* (using a novel generated *UAS-colA* line) under the control of *pnos_GAL4/GCN4_bcd 3′ UTR*. (J) The bZIP factor CncB attenuates Collier–DNA binding complex formation: increasing amount of CncB causes a decrease in C1 (ColA/ColB) complex formation. A probe encompassing the Collier binding site (Fig. S1C), extended in the 3′, was used: CGGCAGCAATTCCCCAATGGCATTTCACTTAGAT. Underlined are the four nucleotides of the imperfect mismatch of the binding consensus of CncB (KTCAT; Veraksa et al., 2000). Both Collier A and Collier B are included in equal volumes in the binding reactions. (K) Sequestering effect of the bZIP factor CncB on Collier DNA-binding activity. Collier–DNA complex formation C1 (ColA/ColB) was allowed to reach the binding equilibrium and then challenged with a constant amount of CncB. Incubation for gradually longer time periods prior to gel loading leads to a decrease in C1. For this particular experiment, the dissociation rate in terms of $t_{1/2}$ was calculated at ~57 sec. ($t_{1/2} = \ln 2/k_{off}$, $k_{off} = -\ln(Fb,t/Fb,0)/t$, k_{off}, dissociation constant). (L) *In vitro* coimmunoprecipitation assay using rabbit-anti-HA (specific IP) or rabbit-anti-bgal (mock IP) on HAN-CncB/ColA (lanes 1–3) and HAN-CncB/ColB (lanes 4–6) input. The western blot was incubated with anti-Col to detect Collier A (lanes 1–3) or Collier B (lanes 4–6) (~62 kDa). Weak Collier detection in the mock IP eluates is due to residual unspecific binding to the beads. (M) Schematic representation of regulatory interactions in the context of a simplified segmentation scheme (adapted from Crozatier et al., 1999). Data reported here indicate that *col* directly activates *hh* in the posterior part of the intercalary segment. Expression of *cnc* in the anterior most part of the mandibular segment during germ band extension is also under positive regulation by *col* (orange dashed arrow; Seecoomar et al., 2000). A secondary spot of *cnc* expression is initiated by *col* during stage 10 in the *hh* expressing cells of the posterior part of the intercalary segment (grey arrow; Crozatier et al., 1999). Our data suggest that the physical protein interaction detected between Collier and CncB may be implicated in attenuating the transcriptional activator function of Collier on the intercalary *hh* expression (red repression bars), to first restrict expression to the posterior part of the intercalary segment and then diminish this expression at a later stage (late 10/11).

the very N-terminus, predicted with the highest threshold value (Ren et al., 2009). Apart from antagonizing ubiquitin-mediated degradation and modifying transcriptional activation/repression potential of transcription factors, sumoylation has also been implicated in protein nucleo-cytoplasmic translocation (reviewed in Du et al., 2008; Zhao, 2007 and references therein; Liu and Gerace, 2009). Alternatively, in the absence of a nuclear localization signal, Collier import in the nucleus may be realized by heterodimerization with a protein that carries an NLS. This would increase the probability that Collier is recruited into combinatorial control mechanisms, which has already been implicated in muscle specification (Dubois et al., 2007). Furthermore, nuclear accumulation of CncB, in converse to a relatively low concentration of

nuclear Collier protein, indicated by the fluorescent immunostainings, may facilitate the sequestering function of CncB to antagonize and overcome the DNA-binding activity of Collier on the *ic-CRE* in the cells of the anterior most part of the mandibular segment during the establishment of procephalic *hh* expression, and at later stages in the *hh* expressing cells of the intercalary lobes.

In this respect it is interesting to note that despite the intrinsic transcriptional activation properties of the Cnc homologs, CncB acts to suppress both the expression and the homeotic selector (maxillary structures promoting) function of *Deformed* (*Dfd*) in the mandibular segment (McGinnis et al., 1998; Mohler et al., 1995). In particular, CncB represses the maintenance phase of *Dfd* transcription in the mandibular cells, most probably by interfering with the positive regulatory function of Deformed within the *Dfd* autoactivation circuit (McGinnis et al., 1998; Veraksa et al., 2000; Zeng et al., 1994). Overexpression of CncB partially represses Dfd-responsive transcriptional target elements *in vivo* (McGinnis et al., 1998). Interestingly, Veraksa et al. (2000) report an interaction between CncB and Dfd proteins in GST pull-downs. Perhaps the negative regulation of *Dfd* expression and function caused by CncB results from CncB interfering with Dfd binding to its cognate target *cis*-regulatory elements *in vivo*, as a consequence of a direct physical interaction at protein level with a sequestering effect similar to the interaction with Collier reported here.

Conclusions

The isolation of an intercalary-specific *cis*-regulatory element from the *hh* upstream region supports a unique mode for anterior head segment-specific transcriptional control of segment polarity gene expression (Ntini and Wimmer, 2011). Thus, not only cross-regulatory interactions among segment polarity genes during the maintenance phase (Gallitano-Mendel and Finkelstein, 1997), but also the initial establishment of procephalic segment polarity gene expression seems to be unique for each of the anterior head segments. The previously proposed mode of second order regulation in anterior head patterning (Crozatier et al., 1999), resulting in activation of *hh* in the posterior part of the intercalary segment, is mediated by the HLH-COE factor Collier evidently via direct DNA binding. The reported physical interaction between Collier and CncB is likely to attenuate the activating function of Collier in the *hh* expressing cells of the posterior part of the intercalary segment at a later developmental stage (Fig. 5M), and it might also be involved in eliminating the potential of target activation by Collier in the anterior most part of the mandibular segment where the two factors are co-expressed.

Supplementary materials related to this article can be found online at doi:10.1016/j.ydbio.2011.09.035.

Acknowledgments

We would like to thank Michele Calos, Stanford University, for the *pTA-attB* plasmid, Johannes Bischof, University of Zurich for providing us with fly lines of the site-specific integration system, Alain Vincent, University Paul Sabatier, Toulouse, for the col^1 mutant fly line as well as the anti-Col antibody, William McGinnis, University of California, San Diego, for the UAS-CncB fly line, the cnc^{VL110} mutant line as well as the anti-Cnc antibody, and Steven Johnsen, Göttingen, for advice on ChIP and real time PCR experiments. This work has been supported by the European Community's Marie Curie Research Training Network *ZOONET* under contract MRTN-CT-2004-005624 (to EAW).

References

Abzhanov, A., Kaufman, T.C., 1999. Homeotic genes and the arthropod head: expression patterns of the *labial*, *proboscipedia*, and *Deformed* genes in crustaceans and insects. Proc. Natl. Acad. Sci. U. S. A. 96, 10224–10229.

Bejerano, G., Siepel, A.C., Kent, W.J., Haussler, D., 2005. Computational screening of conserved genomic DNA in search of functional noncoding elements. Nat. Methods 2, 535–545.

Bischof, J., Maeda, R.K., Hediger, M., Karch, F., Basler, K., 2007. An optimized transgenesis system for *Drosophila* using germ-line-specific phiC31 integrases. Proc. Natl. Acad. Sci. U. S. A. 104, 3312–3317.

Brand, A.H., Perrimon, N., 1993. Targeted gene expression as a means of altering cell fates and generating dominant phenotypes. Development 118, 401–415.

Campos-Ortega, J.A., Hartenstein, V., 1997. The embryonic development of *Drosophila melanogaster*, 2nd edition. Springer-Verlag Berlin Heidelberg, Germany.

Carey, M., Smale, T., 2000. Determining the K_d of a protein using EMSA and oligonucleotide competition. Transcriptional Regulation in Eukaryotes. Cold Spring Harbor Laboratory Press, Cold Spring Harbor, New York, USA, pp. 263–265.

Cartharius, K., Frech, K., Grote, K., Klocke, B., Haltmeier, M., Klingenhoff, A., Frisch, M., Bayerlein, M., Werner, T., 2005. MatInspector and beyond: promoter analysis based on transcription factor binding sites. Bioinformatics 21, 2933–2942.

Chipman, A.D., Akam, M., 2008. The segmentation cascade in the centipede *Strigamia maritima*: involvement of the Notch pathway and pair-rule gene homologues. Dev. Biol. 319, 60–169.

Cohen, S.M., Jürgens, G., 1990. Mediation of *Drosophila* head development by gap-like segmentation genes. Nature 346, 482–485.

Cohen, S., Jürgens, G., 1991. *Drosophila* headlines. Trends Genet. 7, 267–272.

Cokol, M., Nair, R., Rost, B., 2000. Finding nuclear localization signals. EMBO Rep. 1, 411–415.

Crozatier, M., Valle, D., Dubois, L., Ibnsouda, S., Vincent, A., 1996. Collier, a novel regulator of *Drosophila* head development, is expressed in a single mitotic domain. Curr. Biol. 6, 707–718.

Crozatier, M., Valle, D., Dubois, L., Ibnsouda, S., Vincent, A., 1999. Head versus trunk patterning in the *Drosophila* embryo; *collier* requirement for formation of the intercalary segment. Development 126, 4385–4394.

Daburon, V., Mella, S., Plouhinec, J.L., Mazan, S., Crozatier, M., Vincent, A., 2008. The metazoan history of the COE transcription factors. Selection of a variant HLH motif by mandatory inclusion of a duplicated exon in vertebrates. BMC Evol. Biol. 8, 131.

Damen, W.G., 2002. Parasegmental organization of the spider embryo implies that the parasegment is an evolutionary conserved entity in arthropod embryogenesis. Development 129, 1239–1250.

Diederich, R.J., Merrill, V.K., Pultz, M.A., Kaufman, T.C., 1989. Isolation, structure, and expression of labial, a homeotic gene of the antennapedia complex involved in *Drosophila* head development. Genes Dev. 3, 399–414.

Dietzl, G., Chen, D., Schnorrer, F., Su, K.C., Barinova, Y., Fellner, M., Gasser, B., Kinsey, K., Oppel, S., Scheiblauer, S., Couto, A., Marra, V., Keleman, K., Dickson, B.J., 2007. A genome-wide transgenic RNAi library for conditional gene inactivation in *Drosophila*. Nature 448, 151–156.

Dray, N., Tessmar-Raible, K., Le Gouar, M., Vibert, L., Christodoulou, F., Schipany, K., Guillou, A., Zantke, J., Snyman, H., Béhague, J., Vervoort, M., Arendt, D., Balavoine, G., 2010. Hedgehog signaling regulates segment formation in the annelid Platynereis. Science 329, 339–342.

Du, J.X., Bialkowska, A.B., McConnell, B.B., Yang, V.W., 2008. SUMOylation regulates nuclear localization of Krüppel-like factor 5. J. Biol. Chem. 283, 31991–32002.

Dubois, L., Enriquez, J., Daburon, V., Crozet, F., Lebreton, G., Crozatier, M., Vincent, A., 2007. Collier transcription in a single *Drosophila* muscle lineage: the combinatorial control of muscle identity. Development 134, 4347–4355.

Finkelstein, R., Perrimon, N., 1991. The molecular genetics of head development in *Drosophila melanogaster*. Development 112, 899–912.

Gallitano-Mendel, A., Finkelstein, R., 1997. Novel segment polarity gene interactions during embryonic head development in *Drosophila*. Dev. Biol. 192, 599–613.

Gallitano-Mendel, A., Finkelstein, R., 1998. Ectopic *orthodenticle* expression alters segment polarity gene expression but not head segment identity in the *Drosophila* embryo. Dev. Biol. 199, 125–137.

Grossniklaus, U., Cadigan, K.M., Gehring, W.J., 1994. Three maternal coordinate systems cooperate in the patterning of the *Drosophila* head. Development 120, 3155–3171.

Hagman, J., Gutch, M.J., Lin, H., Grosschedl, R., 1995. EBF contains a novel zinc coordination motif and multiple dimerization and transcriptional activation domains. EMBO J. 14, 2907–2916.

Holland, L.Z., Kene, M., Williams, N.A., Holland, N.D., 1997. Sequence and embryonic expression of the amphioxus *engrailed* gene (AmphiEn): the metameric pattern of transcription resembles that of its segment-polarity homolog in *Drosophila*. Development 124, 723–1732.

Jackson, D.J., Meyer, N.P., Seaver, E., Pang, K., McDougall, C., Moy, V.N., Gordon, K., Degnan, B.M., Martindale, M.Q., Burke, R.D., Peterson, K.J., 2010. Developmental expression of COE across the Metazoa supports a conserved role in neuronal cell-type specification and mesodermal development. Dev. Genes Evol. doi:10.1007/s00427-010-0343-3.

Janody, F., Reischl, J., Dostatni, N., 2000. Persistence of Hunchback in the terminal region of the *Drosophila* blastoderm embryo impairs anterior development. Development 127, 1573–1582.

Liu, G.H., Gerace, L., 2009. Sumoylation regulates nuclear localization of lipin-1alpha in neuronal cells. PLoS One 4, e7031.

Loots, G., Ovcharenko, I., Pachter, L., Dubchak, I., Rubin, E., 2002. rVISTA for comparative sequence-based discovery of functional transcription factor binding sites. Genome Res. 12, 832–839.

Mavrakis, M., Rikhy, R., Lilly, M., Lippincott-Schwartz, J., 2008. Fluorescence imaging techniques for studying *Drosophila* embryo development. Curr. Protoc. Cell Biol. 39, 4.18.1–4.18.43.

McGinnis, W., Krumlauf, R., 1992. Homeobox genes and axial patterning. Cell 68, 283–302.
McGinnis, N., Ragnhildstveit, E., Veraksa, A., McGinnis, W., 1998. A cap 'n' collar protein isoform contains a selective Hox repressor function. Development 125, 4553–4564.
Merrill, V.K., Diederich, R.J., Turner, F.R., Kaufman, T.C., 1989. A genetic and developmental analysis of mutations in labial, a gene necessary for proper head formation in *Drosophila* melanogaster. Dev. Biol. 135, 376–391.
Mohler, J., 1995. Spatial regulation of segment polarity gene expression in the anterior terminal region of the *Drosophila* blastoderm embryo. Mech. Dev. 50, 151–161.
Mohler, J., Mahaffey, J.W., Deutsch, E., Vani, K., 1995. Control of *Drosophila* head segment identity by the bZIP homeotic gene *cnc*. Development 121, 237–247.
Mohler, J., Seecoomar, M., Agarwal, S., Bier, E., Hsai, J., 2000. Activation of *knot* (*kn*) specifies the 3–4 intervein region in the *Drosophila* wing. Development 127, 55–63.
Ntini, E., Wimmer, E.A., 2011. Unique establishment of procephalic head segments is supported by the identification of *cis*-regulatory elements driving segment-specific segment polarity gene expression in *Drosophila*. Dev. Genes Evol. 221, 1–16.
Patel, N.H., 1994. Developmental evolution: insights from studies of insect segmentation. Science 266, 581–590.
Pozzoli, O., Bosetti, A., Croci, L., Consalez, G.G., Vetter, M.L., 2001. Xebf3 is a regulator of neuronal differentiation during primary neurogenesis in *Xenopus*. Dev. Biol. 233, 495–512.
Ramos, D.M., Kamal, F., Wimmer, E.A., Cartwright, A.N., Monteiro, A., 2006. Temporal and spatial control of transgene expression using laser induction of the *hsp70* promoter. BMC Dev. Biol. 6, 55.
Rehm, E.J., Hannibal, R.L., Chaw, R.C., Vargas-Vila, M.A., Patel, N.H., 2009. *In situ* hybridization of labeled RNA probes to fixed *Parhyale hawaiensis* embryos. CSH Protoc.. doi:10.1101/pdb.prot5130
Ren, J., Gao, X., Jin, C., Zhu, M., Wang, X., Shaw, A., Wen, L., Yao, X., Xue, Y., 2009. Systematic study of protein sumoylation: development of a site-specific predictor of SUMOsp 2.0. Proteomics 9, 3409–3412.
Rogers, B.T., Kaufman, T.C., 1996. Structure of the insect head as revealed by the EN protein pattern in developing embryos. Development 122, 3419–3432.
Rogers, B.T., Kaufman, T.C., 1997. Structure of the insect head in ontogeny and phylogeny: a view from *Drosophila*. Int. Rev. Cytol. 174, 1–84.
Sandmann, T., Jakobsen, J.S., Furlong, E.E., 2006. ChIP-on-chip protocol for genome-wide analysis of transcription factor binding in *Drosophila melanogaster* embryos. Nat. Protoc. 1, 2839–2855.
Schmidt-Ott, U., Technau, G.M., 1992. Expression of *en* and *wg* in the embryonic head and brain of *Drosophila* indicates a refolded band of seven segment remnants. Development 116, 11–125.
Schmidt-Ott, U., González-Gaitán, M., Jäckle, H., Technau, G.M., 1994a. Number, identity, and sequence of the *Drosophila* head segments as revealed by neural elements and their deletion patterns in mutants. Proc. Natl. Acad. Sci. U. S. A. 91, 8363–8367.
Schmidt-Ott, U., Sander, K., Technau, G., 1994b. Expression of *engrailed* in embryos of a beetle and five dipteran species with special reference to the terminal regions. Roux's Arch. Dev. Biol. 203, 298–303.
Schöck, F., Reischl, J., Wimmer, E., Taubert, H., Purnell, B.A., Jäckle, H., 2000. Phenotypic suppression of empty spiracles is prevented by *buttonhead*. Nature 405, 351–354.
Seecoomar, M., Agarwal, S., Vani, K., Yang, G., Mohler, J., 2000. *knot* is required for the hypopharyngeal lobe and its derivatives in the *Drosophila* embryo. Mech. Dev. 91, 209–215.
Segal, E., Raveh-Sadka, T., Schroeder, M., Unnerstall, U., Gaul, U., 2008. Predicting expression patterns from regulatory sequence in *Drosophila* segmentation. Nature 451, 535–540.
Smith, C.L., 2001. Basic confocal microscopy. Curr. Protoc. Cell Biol. 00 2C.1.1–2C.1.19.
St Johnston, D., Nüsslein-Volhard, C., 1992. The origin of pattern and polarity in the *Drosophila* embryo. Cell 68, 201–219.
Sullivan, W., Ashburner, M., Scott Hawley, R., 2000. Preparation of nuclear extracts from *Drosophila* embryos. Drosophila Protocols. Cold Spring Harbor Laboratory Press, Cold Spring Harbor, New York, USA, pp. 553–557.
Swevers, L., Cherbas, L., Cherbas, P., Iatrou, K., 1996. Bombyx EcR (BmEcR) and Bombyx USP (BmCF1) combine to form a functional ecdysone receptor. Insect Biochem. Mol. Biol. 26, 217–221.
Veraksa, A., McGinnis, N., Li, X., Mohler, J., McGinnis, W., 2000. Cap 'n' collar B cooperates with a small Maf subunit to specify pharyngeal development and suppress deformed homeotic function in the *Drosophila* head. Development 127, 4023–4037.
Vincent, A., Blankenship, J.T., Wieschaus, E., 1997. Integration of the head and trunk segmentation systems controls cephalic furrow formation in *Drosophila*. Development 124, 3747–3754.
Wang, M.M., Tsai, R.Y., Schrader, K.A., Reed, R.R., 1993. Genes encoding components of the olfactory signal transduction cascade contain a DNA binding site that may direct neuronal expression. Mol. Cell. Biol. 13, 5805–5813.
Wimmer, E.A., Cohen, S.M., Jäckle, H., Desplan, C., 1997. *Buttonhead* does not contribute to a combinatorial code proposed for *Drosophila* head development. Development 124, 1509–1517.
Wodarz, A., 2008. Extraction and immunoblotting of proteins from embryos. Methods Mol. Biol. 420, 335–345.
Zeng, C., Pinsonneault, J., Gellon, G., McGinnis, N., McGinnis, W., 1994. Deformed protein binding sites and cofactor binding sites are required for the function of a small segment-specific regulatory element in *Drosophila* embryos. EMBO J. 13, 2362–2377.
Zhao, J., 2007. Sumoylation regulates diverse biological processes. Cell. Mol. Life Sci. 64, 3017–3033.